Universidad Politécnica de Madrid

Escuela Técnica Superior de Ingenieros de Caminos, Canales y Puertos

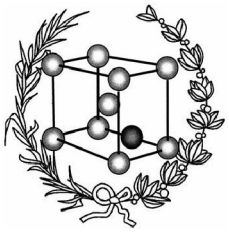

ScAlN based SAW devices with embedded IDT

Proyecto de fin de carrera

Diego López de Bustos

Grado de Ingeniero de Materiales

Directores:

Gonzalo Fuentes Iriarte

Miguel Sinusía Lozano

2019

A mi familia y amigos

Agradecimientos

Agradecer a Gonzalo Fuentes la oportunidad de poder realizar este proyecto.

Agradecer a David López y demás personal del ISOM por haberme ayudado siempre que lo he necesitado.

Y por último agradecer a Miguel Sinusía todas las horas que ha dedicado a este proyecto y su paciencia conmigo.

Resumen

El objetivo de este proyecto ha sido la mejora del factor de acoplamiento electromecánico en dispositivos de ondas acústicas de superficie. Esta mejora se ha llevado a cabo mediante el enterramiento del transductor interdigital (IDT) en una capa de nitruro de escandio aluminio (ScAlN).

Para realizar este objetivo se ha llevado a cabo la optimización de un ataque húmedo con ácido fosfórico (H_3PO_4) a ScAlN y el cálculo de la curva de Arrhenius correspondiente a susodicha reacción, paso necesario para la fabricación de los dispositivos. A continuación, se han fabricado los dispositivos mediante un proceso de microfabricación que engloba "sputtering", metalización, nanolitografía y el mencionado ataque húmedo. Finalmente, se ha medido y analizado la diferencia de propiedades de estos dispositivos antes y después de enterrar el IDT.

Abstract

The objective of this project has been the enhancement of the electromechanical coupling factor in surface acoustic waves (SAW) devices. This enhancement has been accomplished by embedding the interdigital transducer (IDT) in a layer of scandium aluminum nitride (ScAlN).

To reach this objective the optimization of the wet etching of ScAlN with phosphoric acid (H_3PO_4) has been carried out, as well as the calculation of the Arrhenius equation of the reaction, necessary step for the fabrication of the devices. Next, the fabrication of devices with a microfabrication process including sputtering, metallization, nanolithography and the mentioned wet etching has been made. Finally, the change in properties of the devices has been measured before and after embedding the IDT.

CONTENTS

FIGURES

TABLES

1 Introduction and objectives

1.1 Introduction

Surface acoustic wave (SAW) devices are widely used in electronic circuits. They have multiple applications as resonators, oscillators, filters and sensors. Nowadays, communication systems are working with larger data fluxes than ever, and 5G technology is being broadly developed. Therefore, these devices must be adapted to new communication systems working at bigger frequencies with larger bandwidths. For this purpose it is essential to improve current SAW devices. [1]

In SAW devices functioning as bandpass filters, the bandwidth highly depends on the electromechanical coupling factor K^2. [2] The need to improve this value is then crucial to make new filters compatible with 5G technology, which will need a larger fractional bandwidth. [3] This improvement can also serve for ultra-wide bandpass filters working at lower frequencies. [4]

The mechanism of SAW devices consists in the transduction from electric energy to mechanical energy, and the other way around. This is accomplished using piezoelectric materials.

When a piezoelectric material is under the influence of an electrical field, it has a mechanical response (it deforms). When a stress is applied to the material, a voltage differential is obtained. This way, an electric current can be used to strain a piezoelectric material obtaining an acoustic pulse, and vice versa. Thus, by placing an interdigital transducer (IDT) in a piezoelectric material, like the scheme shown in Figure 1, SAWs can be excited (input transducer) and detected (output transducer) efficiently.

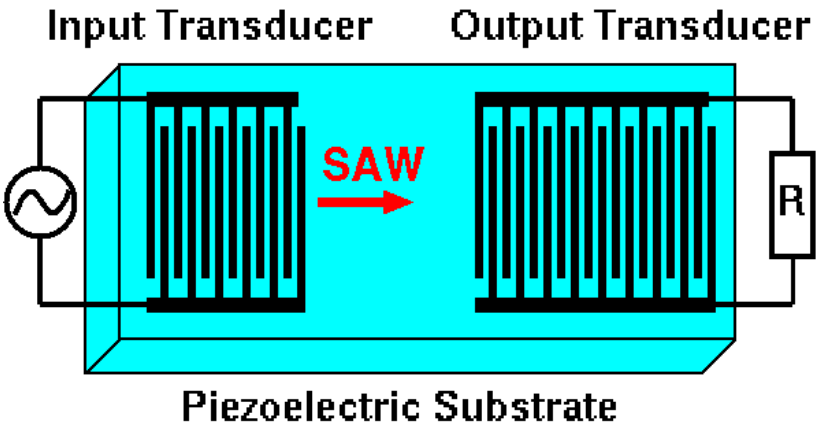

Figure 1. SAW processing device containing two interdigital transducers

The selection of the piezoelectric material is essential for the performance of the SAW device. This is logical, as this material is the medium in which the acoustic wave propagates. Therefore, the elastic modulus and density of the material, among other properties, will determine how the wave propagates.

Thus, the substrate material influences several key SAW properties: SAW velocity (which is proportional to the wave frequency), electromechanical coupling factor, temperature stability, beam steering, propagation loss and permittivity. [5]

The SAW velocity depends on the density and elastic modulus of the substrate material, as it can be seen in the formula (1), known as the Newton - Laplace equation. [6]

$$v = \sqrt{E/\rho} \tag{1}$$

The electromechanical coupling factor K^2 represents how much mechanical energy is converted to electrical energy in a piezoelectric material. This relation can be seen in formula (2). [7]

$$K^2 = E_m/E_e \tag{2}$$

There are several piezoelectric materials to be selected for generating the SAW. Single crystals are the traditional piezoelectric materials: quartz, PZT, $LiNbO_3$, $LiTaO_3$, $Li_2B_4O_7$ or langasite. [5] These materials increase fabrication costs because of the high temperatures needed to deposit them as crystals. Furthermore, these high temperatures would make impossible to make SAW devices compatibles with integrated circuits, like CMOS. [8]

Alternatively to single crystals, thin films can be used to achieve larger wave velocities, specially ZnO and AlN, [5] as these thin films allow us to combine the properties of a piezoelectric material at the top, and a material with great wave propagation properties below, so a significant wave proportion of the wave is propagated in this last material. This makes it possible to use non-piezoelectric materials as the propagation medium.

Diamond is one of these possible materials, used mainly because of its very high acoustic wave velocity, which is the highest among all solids. [9]

As it was previously commented, it is essential to make devices compatible with new technologies, particularly with 5G. Thus, apart from the bandwidth per se, it is also crucial for the center frequency of these devices to be higher. [10] Using diamond, the highest possible frequencies are aimed for.

Compared with ZnO/Diamond structures, AlN/Diamond structures have a lower velocity dispersion, because of a smaller difference between the two materials (AlN and diamond) SAW phase velocity. [11] AlN is subsequently the preferable thin film when using diamond.

AlN has excellent electroacoustic properties, as well as a high Curie temperature (1150ºC), which allows us to use this material in high temperatures. However, materials with a high Curie temperature (T_c) normally have low piezoelectric coefficients, as normally these coefficients become more pronounced as T_c is approached. [12] This is the case for AlN, with a piezoelectric modulus d_{33} of 5.5 pC/N, which is lower than other materials like the already mentioned ZnO, PZT or $LiNbO_3$. [13]

However, if the wurtzite structure AlN is alloyed with ScN, the AlN piezoelectric modulus d_{33} can be significantly increased. This was reported in 2009 by Akiyama et al., [14] who showed a 500 % improvement in the piezoelectric modulus d_{33}. Since then several research groups have reported about the electroacoustic properties of ScAlN.

The significant increase of the piezoelectric modulus d_{33} is due to the atomic structural instability provoked by the alloying (the lattice is enlarged). [13] Moreover, researchers have reported a considerable rise in the K^2 value using ScAlN instead of AlN. [10]

Because of all this, in this work ScAlN was used on diamond, concretely a $Sc_{0.43}Al_{0.57}N$ composition was synthesized. Such composition is reported to maximize the piezoelectric properties, as it can be seen in Figure 2. [15]

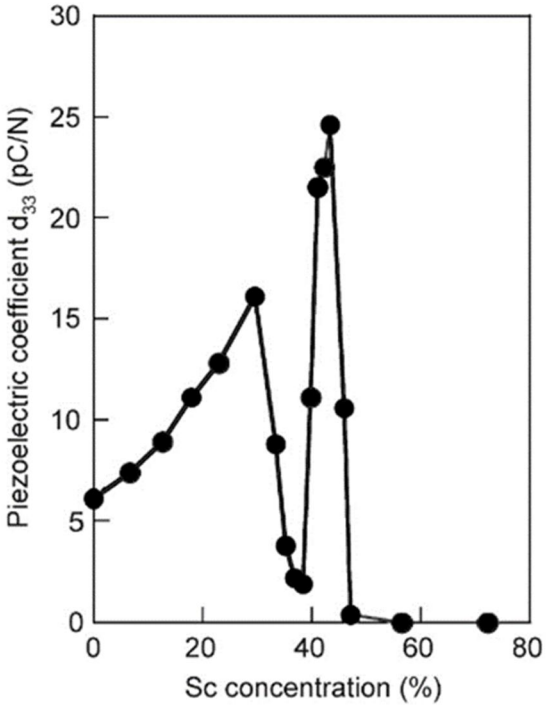

Figure 2. Dependence of piezoelectric coefficient d_{33} of ScAlN alloys on Sc concentration [14]

The relative position of the IDT with regards to the piezoelectric thin film and the substrate changes the electrical performance of the SAW device. There are different ways of putting the IDT in the structure, as it is seen in Figure 3.

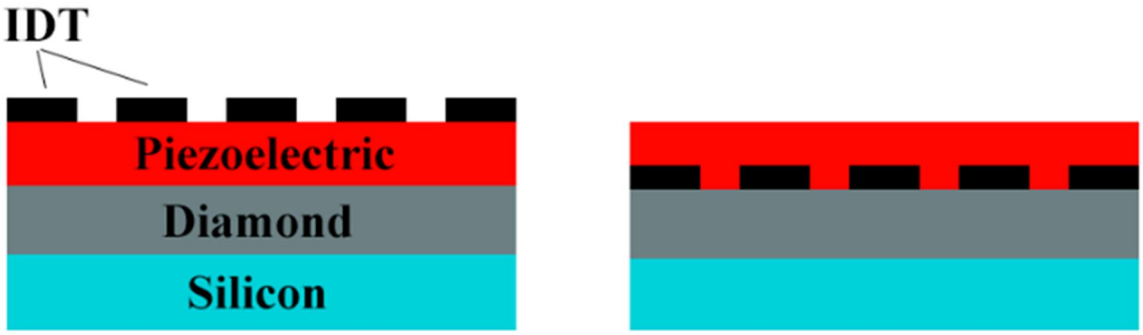

Figure 3. SAW device with the IDT above the piezoelectric layer (left) and embedded in it (right)

If the IDT is embedded in the piezoelectric material, and not above it, theoretically the electromechanical coupling factor K^2 improves. [10] This improvement has been tested in simulations, as it can be seen in Figure 4 for Rayleigh and Sezawa modes, which are the

first and second resonance modes, respectively. At the author knowledge, that improvement hasn't been empirically reported.

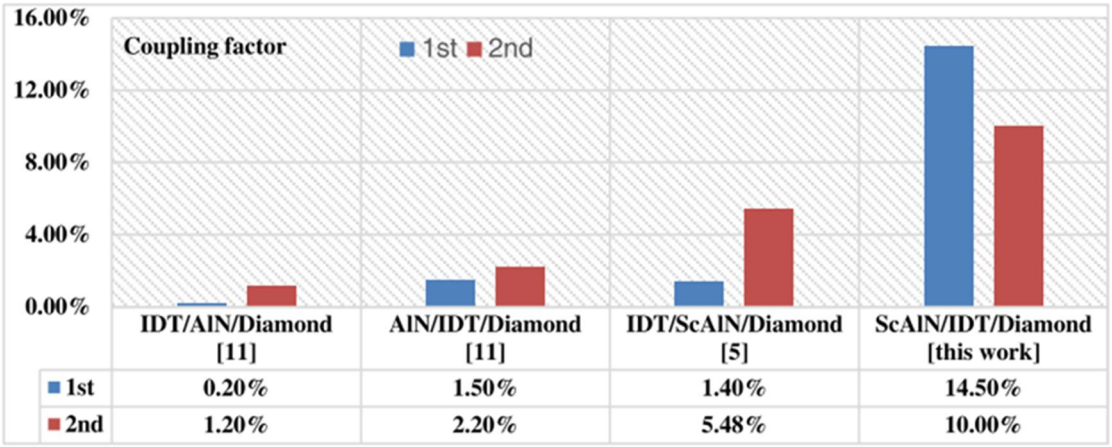

	IDT/AlN/Diamond [11]	AlN/IDT/Diamond [11]	IDT/ScAlN/Diamond [5]	ScAlN/IDT/Diamond [this work]
1st	0.20%	1.50%	1.40%	14.50%
2nd	1.20%	2.20%	5.48%	10.00%

Figure 4. Simulated comparison of maximum K^2 for Rayleigh (1st) and Sezawa (2nd) modes with different layered structure configurations [9]

For the structure in Figure 3 (right), there is no contact with the electrodes, as they are under the piezoelectric layer. That's why it is necessary to "open a window" in the piezoelectric material so the electrodes can be reached, and the electric current can activate the SAW device. This can be done using wet etching.

Wet etching is a widely used technique in microtechnology. It is basically a chemical reaction. This guarantees great selectivity if used properly. Concretely, for ScAlN it can be used a reaction with phosphoric acid (H_3PO_4) which it's known as a good etchant for AlN [16] in a previously selected zone (above the electrode). This zone can be selected using nanolithography.

The mentioned reaction is isotropic (in Figure 5 left). Therefore, the etching rates must be controlled so underetching is not excessive, which could break the devices.

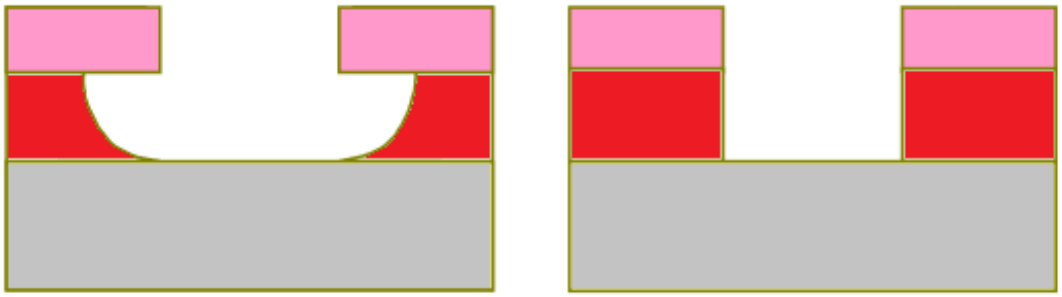

Figure 5. Isotropic (left) and anisotropic (right) wet etching

1.2 Objectives

The objective of this project was to fabricate resonators and filters and test their change in properties before and after embedding the IDT, putting our focus in the possible enhancement of the electromechanical coupling factor K^2.

For this purpose, the experimental part of this work can be divided in two parts. The first one consisted in the optimization of the wet etching of the piezoelectric material (ScAlN) with phosphoric acid, so this reaction could be used later in the fabrication of the devices. For this purpose, it was needed to deposit ScAlN, characterize the material and make the wet etching experiments.

The second one consisted in the fabrication of the devices and the measurement of their properties. For the fabrication, sputtering, nanolithography, metallization and wet etching were used. For the measurement of the device properties, a network analyzer was used before and after embedding the IDT.

After this, both part results were discussed. For the first part the etching rate-temperature curve and the Arrhenius equation plotted. For the second part, the change in properties of the devices was analyzed.

The Institute for Optoelectronic Systems and Microtechnology (ISOM) has years of experience fabricating and characterizing SAW devices. [17][18][19] This experience has

resulted, among other things, in an ongoing collaboration between ISOM and HUAWEI Canada. This project has used the technology and knowledge that has been acquired in this collaboration, and it is thus framed in it.

2 Experimental work

2.1 Synthesis of the ScAlN layer

To start the procedure, ScAlN was grown on the substrate.

First, the substrates had to be cleaned, because impurities degrade the ScAlN c-axis orientation, which is the desired one for piezoelectric properties. The cleaning process began by introducing them in acetone at 330 K for 5 minutes. After this, they were rinsed in methanol at 330 K, which removes acetone residues. The samples stayed in methanol another 5 minutes. During all this process, sonication was used to force the impurities to lift. After taking the samples out of methanol, they were blown dry with N_2.

The process to deposit ScAlN (sputtering) was carried out in a home-built reactive sputtering (Figure 6). It consists of two different chambers, named the synthesis and the load-lock chamber. There are two ways the system dissipates heat in the target: an indium bonded copper backing plate which dissipates heat and water-cooling the target in its backside. The temperature during the synthesis is measured with a thermocouple placed under the substrate holder. This allowed us to verify that temperatures above 100ºC were not recorded.

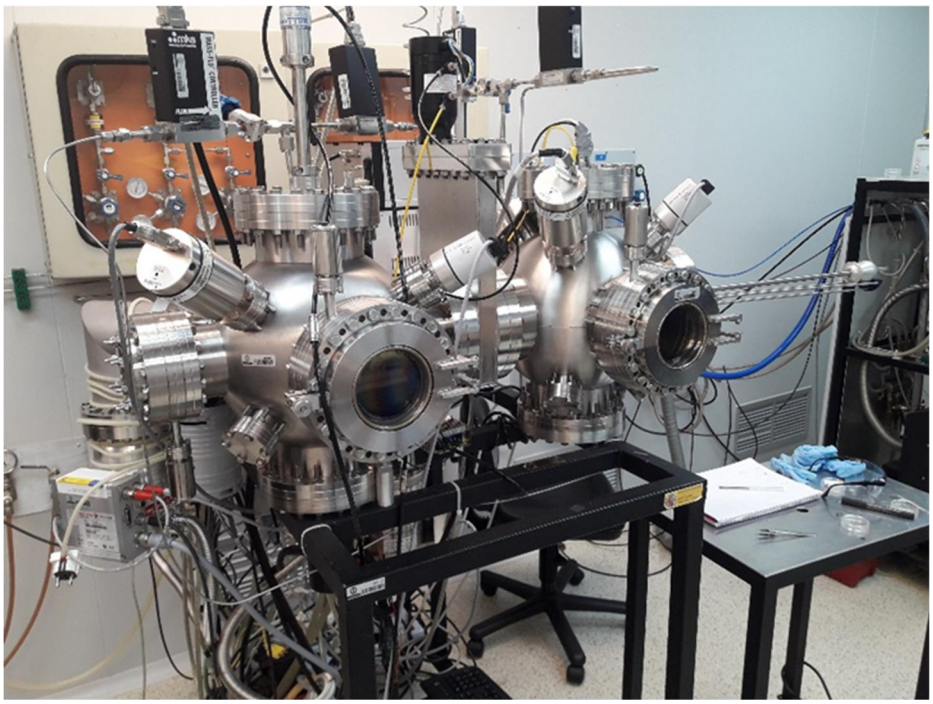

Figure 6. Home-built reactive sputtering equipment

The synthesis chamber is only used for ScAlN synthesis to avoid cross-contamination. The magnetron was powered using an ENI RPG50 asymmetric bipolar-pulsed DC generator with an applied frequency of 250 kHz and a pulse width of 1616 ns. The target-substrate distance was set to 45 mm.

The evolution of the sputtering parameters power, voltage and current during the conditioning and synthesis procedure can be seen in Figure 7.

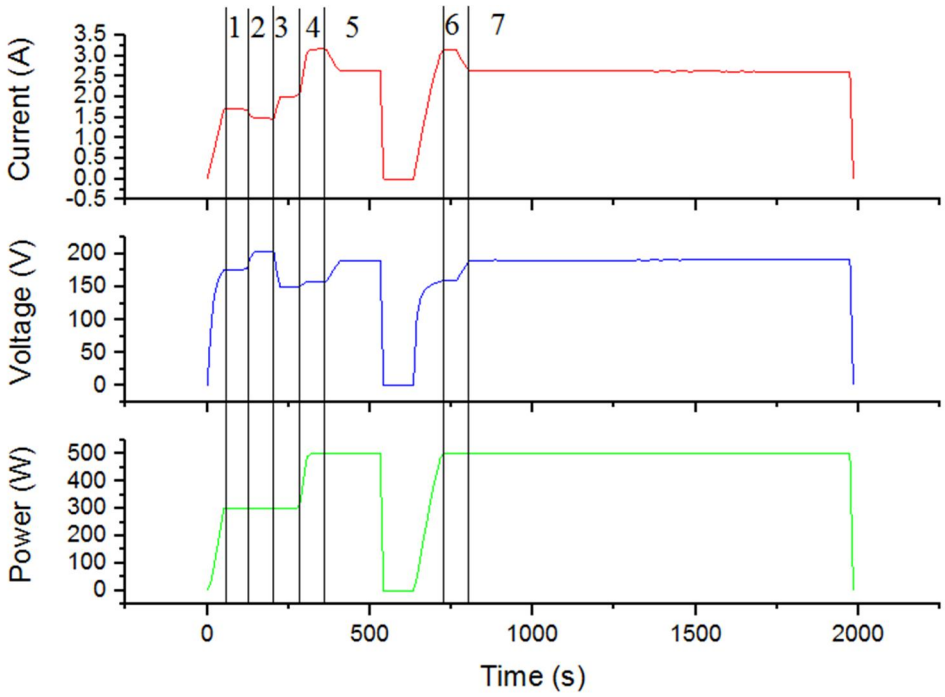

Figure 7. Power, voltage and current evolution during the sputtering process

The conditioning procedure consisted in modifying the gas admixture ratio, the process pressure and the discharge power of the synthesis. As it can be seen in Figure 7, there were six conditionnig steps done. The sputtering paramaters for each step can be seen in Table 1. During step 5 the substrates were transferred from the pre-load chamber to the synthesis chamber with the target shutter closed, and after igniting the plasma during two minutes shutter is removed and the depostion starts

Table 1 Sputtering parameters for each step

Steps	**Process pressure (mTorr)**	**Discharge power (W)**	**Ar flow (sccm)**	**N2 flow (sccm)**	**Gas admixture ratio (%Ar)**
1	30	300	30	0	100
2	10	300	30	0	100
3	10	300	3	9	25
4	10	500	3	9	25
5	3	500	3	9	25
6	3	500	3	9	25
7	3	500	3	9	25

2.2 ScAlN layer characterization by X-Ray diffraction

After the sputtering process, the ScAlN c-axis orientation was verified with x-ray diffraction (XRD). The equipment used was a Phillips X-Pert Pro MRD diffractometer. It can be seen in Figure 8.

Figure 8. Phillips X-Pert Pro MRD diffractometer

Our objective was to check that the ScAlN thin films were highly c-axis oriented. For this purpose, the θ - 2θ scan was done first. This scan is used to detect the crystalline phases presented in our sample including ScAlN, silicon and diamond.

The process consisted in rotating the x-ray generator around θ and the detector along 2θ, going through all incident angles. Every crystalline phase has its constructive angle at some point, which can be calculated with the Bragg law (3). Being "n" a positive integer, "λ" the wavelength, "d" the distance between the crystallographic planes and "θ" the incident angle.

$$n\lambda = 2d \times \sin\theta \tag{3}$$

Once the (0002) ScAlN orientation was checked, which is fundamental to guarantee the piezoelectric behavior of the material, the rocking curves (ω scans) could be done, which are scans that provide quantitative information about a determinate phase orientation within the sample.

This is made by setting the detector at the reflected angle of the studied phase and changing its perpendicular angle (ω). [20] The full width at half maximum (FWHM) of the peak obtained is inversely proportional to the quality of the grains orientation.

The results of these analysis can be seen in section 3.1.

2.3 Wet etching for ScAlN

The profilometer Alpha-Step IQ (Figure 9) was used to verify the piezoelectric layer thickness deposited in the substrate. For that purpose, quartz parts were placed above the samples before the sputtering started, as it can be seen in Figure 10. That way, when these pieces were retired, there was a thickness step between the substrate surface and the deposited thin film ready to be measured.

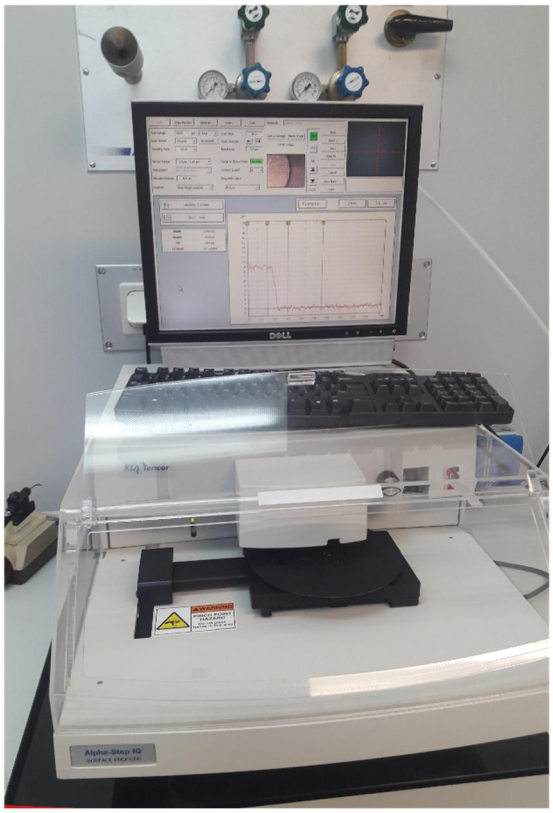

Figure 9. Profilometer Alpha-Step IQ

However, this method created a “shade” near the thickness step. This meant that the thickness step was not abrupt, but gradual. Because of this, it was essential to measure all

the thickness difference with the profilometer. Taking this into account, five different measurements in the profilometer were made.

Figure 10. Si (001) substrates ready to be introduced in the sputtering equipement

With the deposited thickness measured, the wet etching experiments could be started. Phosphoric acid (H_3PO_4) diluted in water (85% acid concentration) was poured in a tube and heated until the sampled temperature. The hot plate used can be seen in Figure 11. When this temperature was stabilized, the sample was rinsed in the acid during a controlled etching time. After that, it was pulled out and introduced in water, which neutralizes the acid.

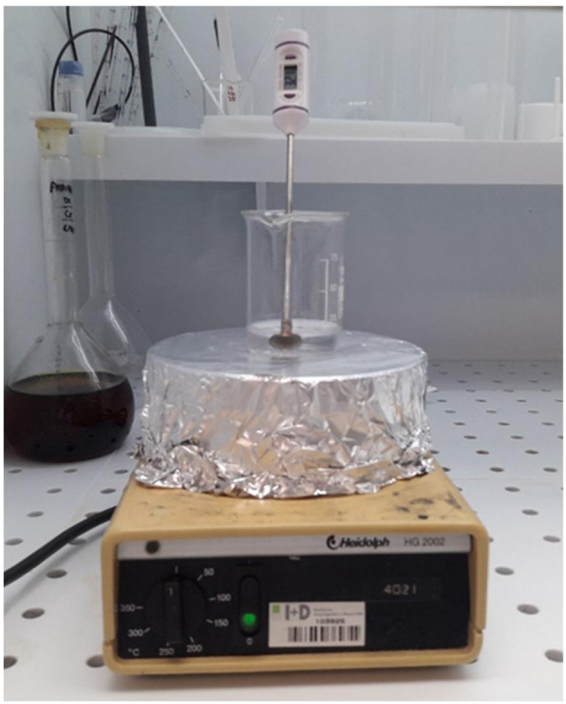

Figure 11. Phosporic acid being heated in the hot plate

This procedure was repeated with five different temperatures: (305.5, 310.5, 315.5, 320.5, 325.5 K). It was decided to measure this temperature range because lower temperatures have an almost negligible etching rate, and higher temperatures can be dangerous because of gas emissions and because they are difficult to control.

Following each wet etching, the thickness was measured again five times with the profilometer, so the thickness difference could be calculated. Dividing the etched thickness between the time that the sample had been rinsed in acid, the etching rate was calculated.

During this process, some difficulties were faced. At first, for security reasons, the thermometer was introduced at first in a water tube that was, theoretically, at the same temperature than the acid. After making several measures this way, the results that were obtained weren't conclusive. The etching rate typical deviation ranged between 20% and 100%, and the curve wasn't coherent with the expected Arrhenius curve.

After this experience, it was suspected that the thermometer wasn't measuring the real acid temperature, so the thermometer was introduced directly in acid and the etching experiment was repeated. After this change, the accuracy of the results improved significantly.

At the end, solving the problems cited above, the five temperatures had been measured, three times each temperature and five measurements with the profilometer for each attack. With this data, the etching rate – temperature graph could be plotted.

2.4 Device fabrication

To start, the diamond substrates were cleaned up with the same cleaning process as described in 2.1 (acetone, methanol and blown dried with N_2). Polycrystalline diamond substrates were used for the resonators, and monocrystalline diamond substrates were used for the filters.

The final structure that was fabricated can be seen in Figure 12.

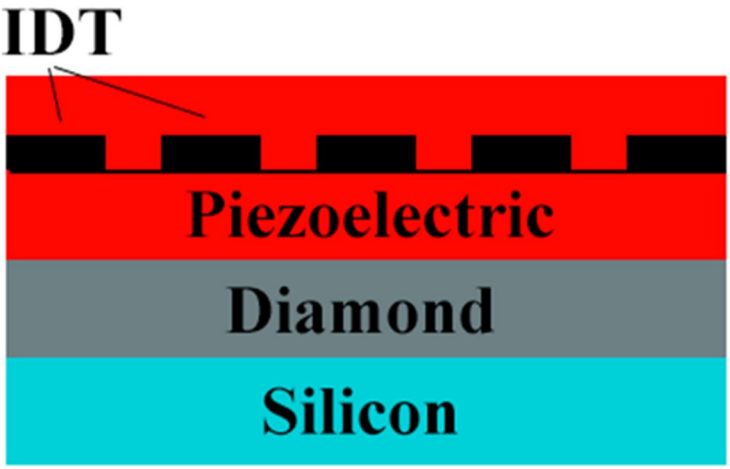

Figure 12. Final structure of the SAW device

The reason for making this structure, and not removing the piezoelectric layer below the IDT as it is shown in the Figure 3 (right), it's that there were difficulties depositing ScAlN above the IDT if there was no piezoelectric material underneath. ScAlN wasn't deposited correctly without a seed layer and this provoked not-working devices. This could be due to stresses in the deposited layer or the lattice mismatch.

After facing these difficulties, it was realized that for the objective of this project, the differences between a device with an IDT above the piezoelectric film, and that same device but with another layer of piezoelectric material deposited above the IDT could be tested as

well. If a K^2 enhancement was accomplished in this case, it was as well proved that the reason was the embedding of the IDT.

Apart from embedding the IDT, the other variable that was inevitably changing was the normalized ScAlN thickness (in both, filters and resonators, the change was 0.11). Normalized thickness is the piezoelectric layer thickness divided by the wavelength of the acoustic wave, which is determined by the IDT. It was known that changing the piezoelectric thickness would change K^2 as well, but in our experience this change is quite low. Simulations done in this matter also confirm this. [21]

Concretely, for our resonators the normalized thickness goes from 0.71 to 0.82. According to the previously referred simulations, this change provokes an absolute change in K^2 of less than 0.01 (1%) for both Rayleigh and Sezawa modes. That's why any significant change in K^2 in this project can be considered due to embedding the IDT.

The first layer of piezoelectric material was deposited with the sputtering equipment, with a thickness goal of 2000 nm for the resonators and 200 nm for the filters.

The reason for this change in thickness as well as the different diamond structures is that the resonators were used to test the fabrication process and the electromechanical coupling factor increase, while the filters were made trying to have as much frequency as possible and less energy losses, which is accomplished by thinning the piezoelectric layer and using monocrystalline diamond respectively. [22]

When this was finished, the nanolithography process was started. First, a spinner was used, which can be seen in Figure 13, to deposit the resist. In this case, a two-resist layer was employed to facilitate the lift-off process. The resists were PMMA and LOR7b.

The procedure was as it follows: the substrate was placed in the center of the spinner, where a vacuum force is then applied. After that, a resist drop was carefully deposited in the substrate and it was spun.

First, the LOR7b resist was deposited diluted in cyclopentanone (2:1 ratio respectively), accomplishing a thickness of 160 nm. After the spinning, a soft bake was applied at 433 K for 2 minutes to remove the dissolvent. Then, the PMMA resist was deposited diluted in chlorobenzene (2:1 ratio), with a thickness of 160 nm. The same soft bake was applied. An organic anti-static layer (Spacer 300Z, Showa Denko) was used to avoid the charge accumulation due to the insulating character of the ScAlN/diamond substrate.

Figure 13. Spinner equipment and the used resists

After that, the sample was introduced in the High-Resolution Electron Beam Lithography System, model CRESTEC CABL-9000C, the equipment shown in Figure 14. Due to the extremely sensible nature of the nanolithography process, this equipment is placed in a special room, in which the light wavelengths are filtered so the photosensitive resists are not affected.

Figure 14. High-Resolution Electron Beam Lithography System CRESTEC CABL-9000C

First, the designs had to be loaded into the system. These can be seen in Figure 15: respectively the resonator and the filter design. After this, the samples could be introduced in the equipment. An electron dose of 200 μC/cm^2 was used.

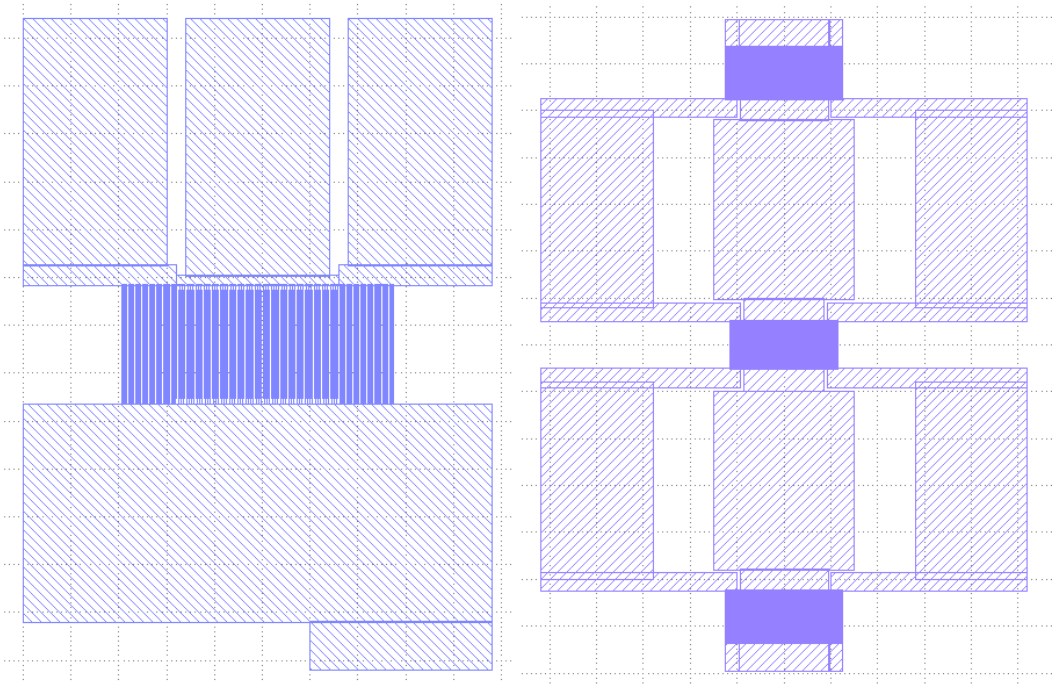

Figure 15. E-beam mask designs used for the resonators (left) and filters (right)

This process was made with positive resists, which means the resist affected by the electron beam is the one developed afterwards. A section of the IDT design seen by a Scanning Electron Microscope (SEM) can be seen in Figure 16.

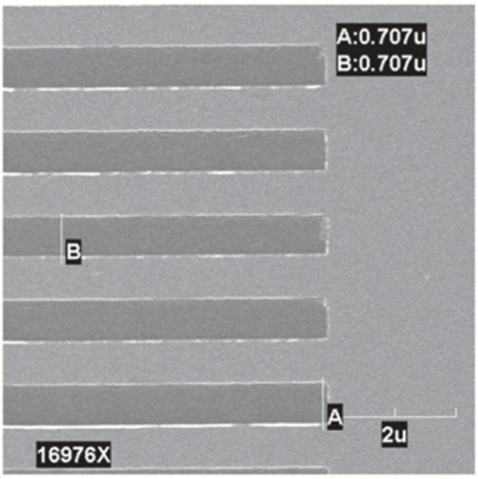

Figure 16. Section of the IDT design seen by a SEM

After the nanolithography process, the development of the resist affected was made with the appropriate developers: AR-P 600-55 for the PMMA resist, and MF319 for the LOR7b resist.

Then, the metallization process was started. The objective was to deposit gold, however, this metal doesn't have good adhesion properties. Therefore, it was needed to deposit a thin layer of chromium (5 nm) first to improve the adhesion. The thickness of the gold layer was 120 nm for the resonators and 65 nm for the filters.

The equipment in which this was made is an Electron Beam Evaporator System Varian-VT 118, as it can be seen in Figure 17.

Figure 17. Electron Beam Evaporator System Varian-VT 118

The nanolithography and metallization process can be seen in Figure 18. The first figure shows the structure when the resists have been deposited. The second is the structure when the resists have been developed. The third is the structure after the metallization process.

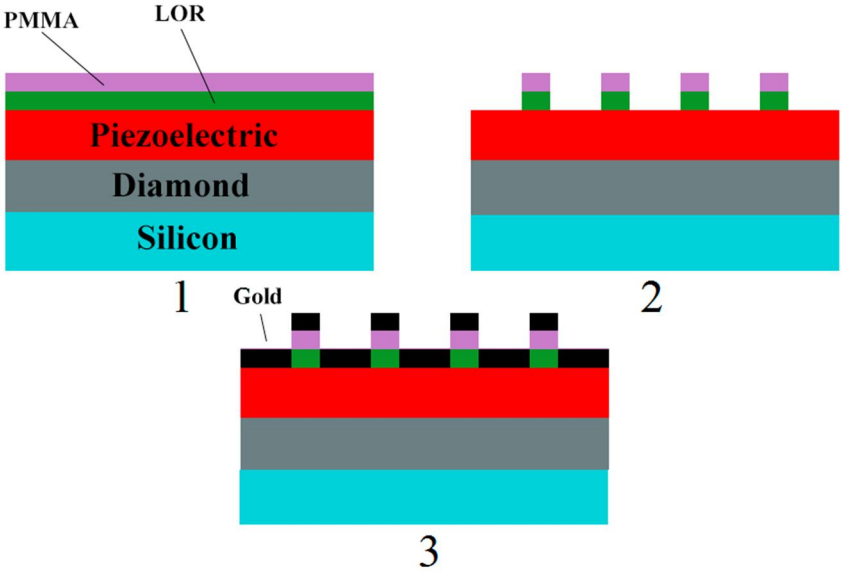

Figure 18. Nanolitography and metallization sucessive structures

Then, the lift off the two resists could be made. They are lifted off using the organic compound N-Methyl-2-pyrrolidone. The resist was introduced in a tube with this compound at 330 K for 5 minutes using sonication. After this, the resist lifted off along with the chromium and gold that was deposited above it. This way, the pattern of the nanolithography made in gold was left. After this, the electrodes and IDT were ready.

During these last steps, it was common to face difficulties. During the lift-off, sometimes part of the gold deposited in the substrate went away as well as it was not well adhered. This left us with not-working devices, so all the process had to be repeated. This happened to us several times.

Adjusting different variables like the resist thickness or the metallization parameters, a highly yielded lift-off was finally accomplished, and the devices were ready to measure before depositing the piezoelectric layer above the IDT. After measuring them, the deposition of the piezoelectric material could be made. The measurement of electrical properties was realized with a network analyzer Agilent N5230 A, which can be seen in Figure 19.

Figure 19. Network analyzer Agilent N5230 A

After this, the second layer of ScAlN could be deposited. The sputtering equipment was used the same way as described in 2.1, but this time with the objective of achieving a thickness of 300 nm for both, resonators and filters. After this, the electrodes and IDT were embedded within the piezoelectric thin film.

All it was needed at this point was to be able to contact the electrodes so the connection could be made. This was made using another nanolithography process. First, the same two resists used before were spun aiming for a thickness of approximately 500 nm each. Then, the "windows" for the electrodes were designed, so the resist develops only on the exposed area to reach the piezoelectric material. This design concept can be seen in Figure 20.

As it can be seen, a reasonable margin from the IDT was left. This is because, as it has ben said before in this work, our wet etching reaction is isotropic, so there is underetching, and thus, there is etched material out of the designed window. Therefore, it had to be made carefully so the ScAlN deposited above the IDT was not reached.

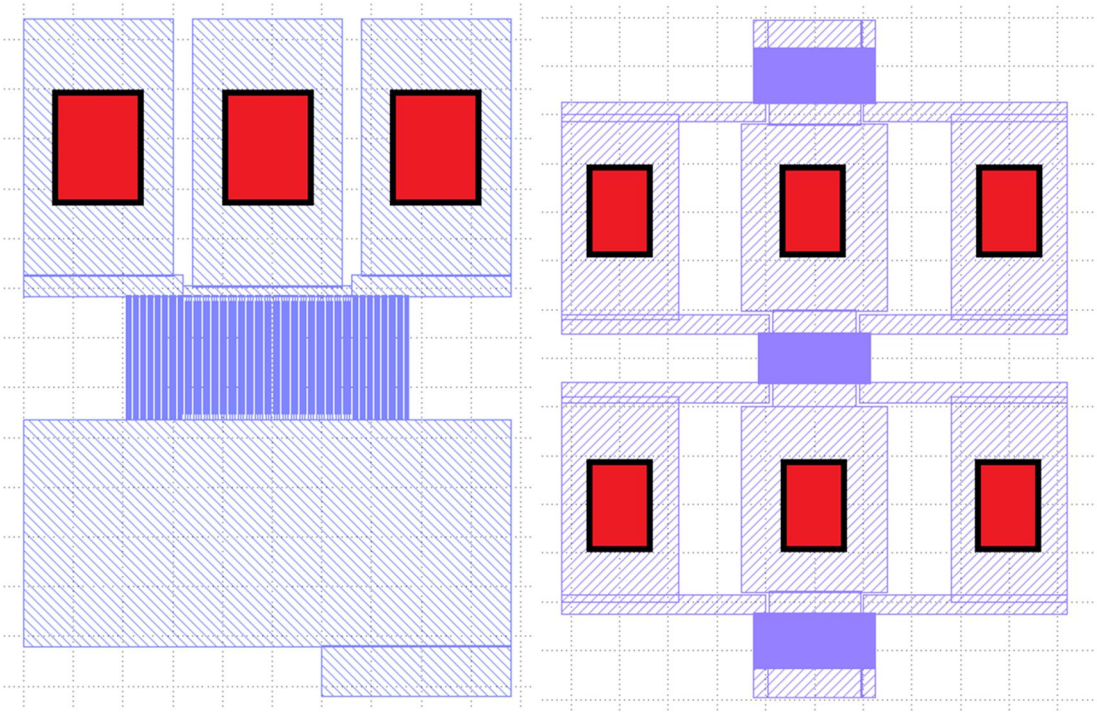

Figure 20. In red, the E-beam mask designs used to open "windows" in the resonators (left) and filters (right)

After having developed the resists with the same developers that were used for the previous nanolithography process, the wet etching could be made, etching the piezoelectric material in the windows and reaching the electrodes. This could be done because the resist is affected by the phosphoric acid at a negligible rate in comparation with ScAlN.

The results obtained in the etching experiments of this work (Section 3.1) for the wet etching were used here. Knowing the etching rate at different temperatures, it was decided to etch ScAlN at 325.5 K for 87 seconds. This time is according to our calculations the minimum time that results in all 300 nm of piezoelectric material etched, so it was used to avoid unnecessary underetching.

After this, and after confirming with the profilometer that all the piezoelectric material was etched, the fabrication of the devices was completed. The final step was to measure them again with the network analyzer previously mentioned and compare the results with the measurements of the device before embedding the electrodes.

3 Results

3.1 ScAlN thin film: XRD

The results of the XRD θ-2θ scan can be seen in Figure 21. As it can be seen, the Si (004) peak is extraordinarily big compared to the rest. This is logical, as Si is a high-quality monocrystalline material. ScAlN peak is at 35.661º, which is the angle in which the rocking curve is made.

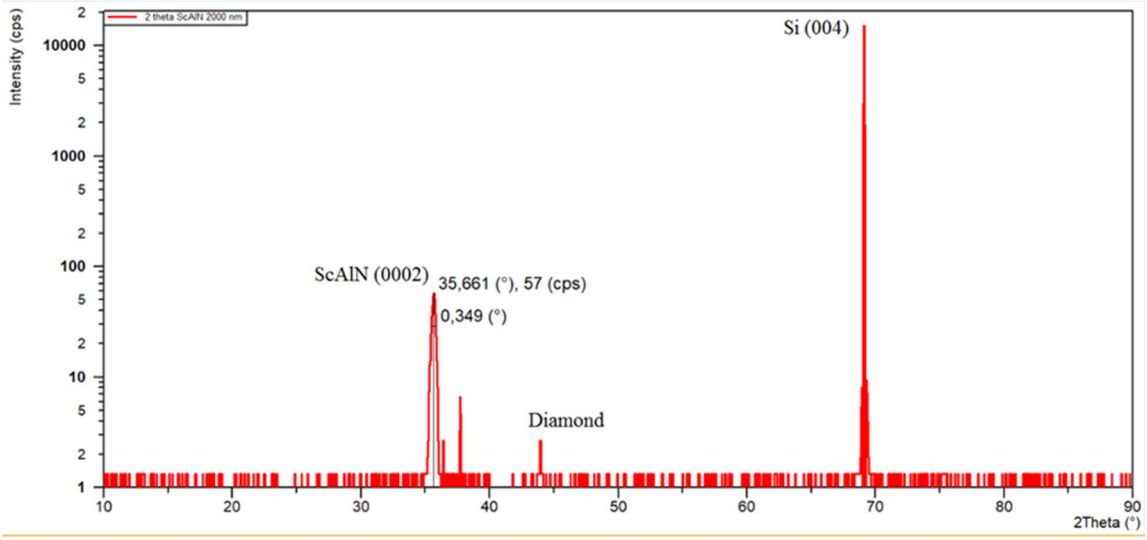

Figure 21. Diffraction pattern of a ScAlN/polycristalline diamond/Si (001) sample

The rocking curve can be seen in Figure 22. The FWHM obtained is 2.64º, which is a small width, and thus it is a good result. Having done this, it was guaranteed that the ScAlN layer deposited was highly c-axis oriented and the project could be proceeded with.

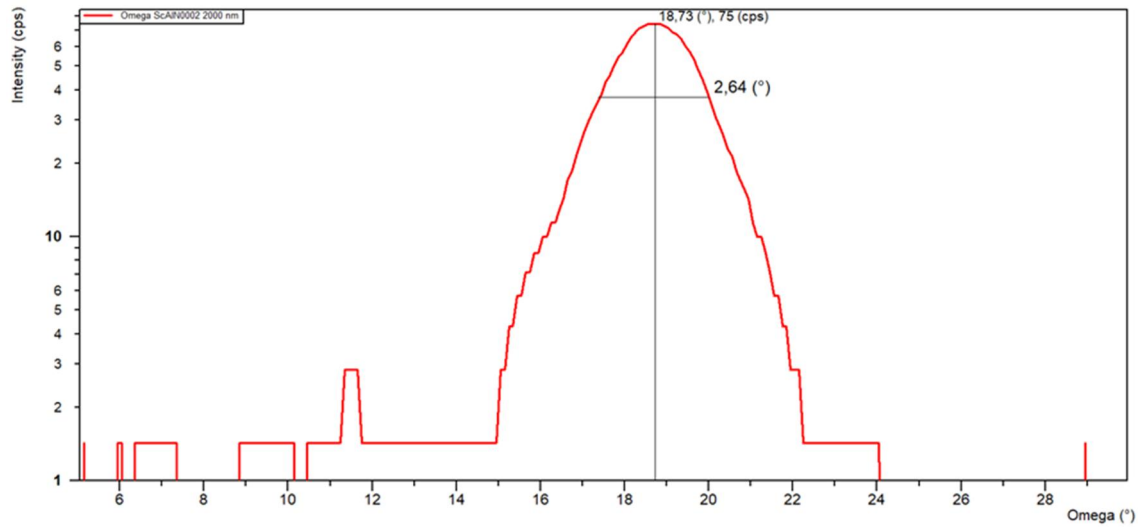

Figure 22. Rocking curve at 35.661º for ScAlN

3.2 ScAlN thin film: Wet etching

In Figure 23 the wet etching rate is plotted as a function of temperature. It follows an Arrhenius curve, as it is typical for chemical reactions. As temperature goes up, so does the number of collisions between the molecules with the minimum activation energy, which provokes an exponential trend.

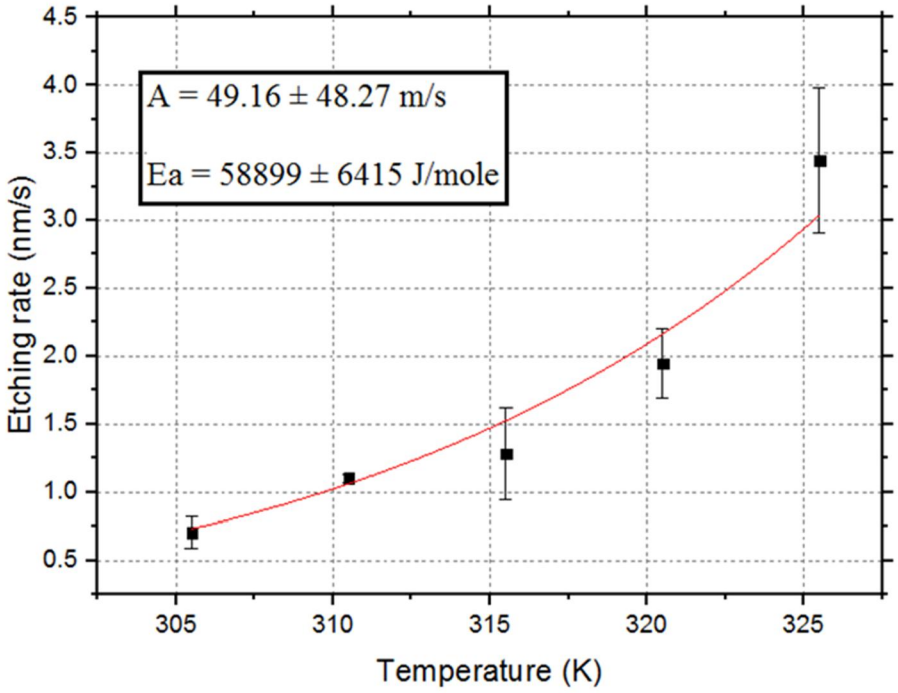

Figure 23. Etching rate vs. temperature plot for wet etching of ScAlN by H_3PO_4

This is explained by the Arrhenius equation (4):

$$k = Ae^{\frac{-E_a}{RT}} \tag{4}$$

Being "k" the rate constant, "A" the pre-exponential factor, "E_a" the activation energy, "R" the universal gas constant and "T" the temperature. It can be observed that the plot is coherent with this equation.

With our data, the Arrhenius constants "Ea" and "A" can be approximately calculated for this concrete reaction. The values obtained can be seen in Figure 23 and they are in the range of referred constant values for other chemical reactions. [23]

3.3 Device characterization

The first devices that were measured were the resonators. The data was analyzed with a Python script, which can be seen in the Appendix. The scattering parameter S_{11} and the admittance parameter Y_{11} vs. frequency plots are the most useful. Both parameters describe the electrical behavior of our devices showing the resonance and antiresonance frequencies.

There were 15 resonators in our sample, but only 8 of them ended up having an electrical response. This could be due to different reasons as ScAlN not having been correctly deposited inside the IDT, or to short-circuited electrodes.

In Figure 24, it can be seen the S_{11} and Y_{11} parameters of one of our working resonators (Resonator A) after embedding the IDT. It was accomplished to propagate several resonance modes, including Rayleigh (1.3 GHz) and Sezawa (2.1 GHz) modes.

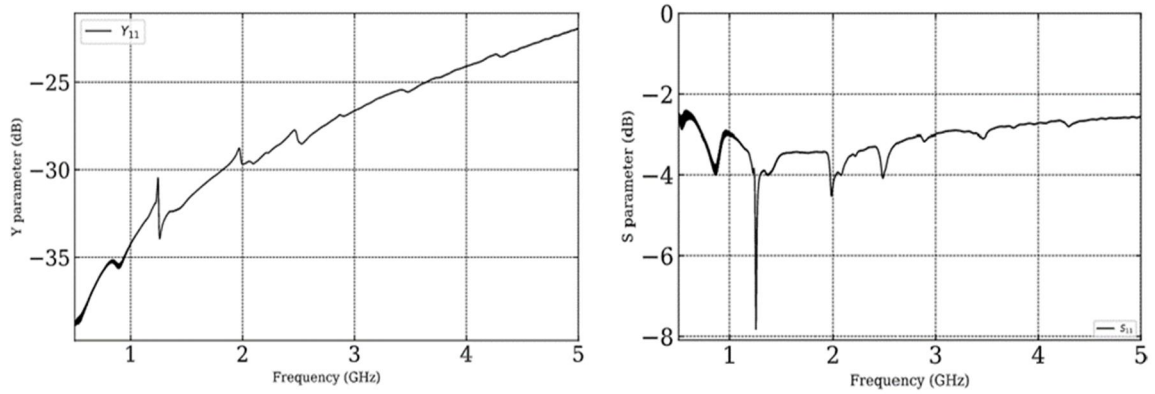

Figure 24. Y_{11} parameter vs. frequency (left) and S_{11} parameter vs. frequency (right) after embedding the IDT

Our objective was to compare the change of K^2 in the first two resonating modes (Rayleigh and Sezawa respectively). Formula (5) was employed to calculate the K^2 of the fabricated resonators: [24]

$$K^2 = (\frac{\pi}{2})^2 \times \left(\frac{fa - fr}{fa}\right) \tag{5}$$

Being "*fa"* the antiresonance frequency or parallel and "*fr*" the resonance frequency or series frequency. As it can be deducted from the equation, K^2 depends on the frequency range between these two values. In Figure 25, these two values can be seen for the Rayleigh mode of the Resonator A, where "*fr"* is when impedance tends to 0 and "*fa"* when impedance tends to infinity.

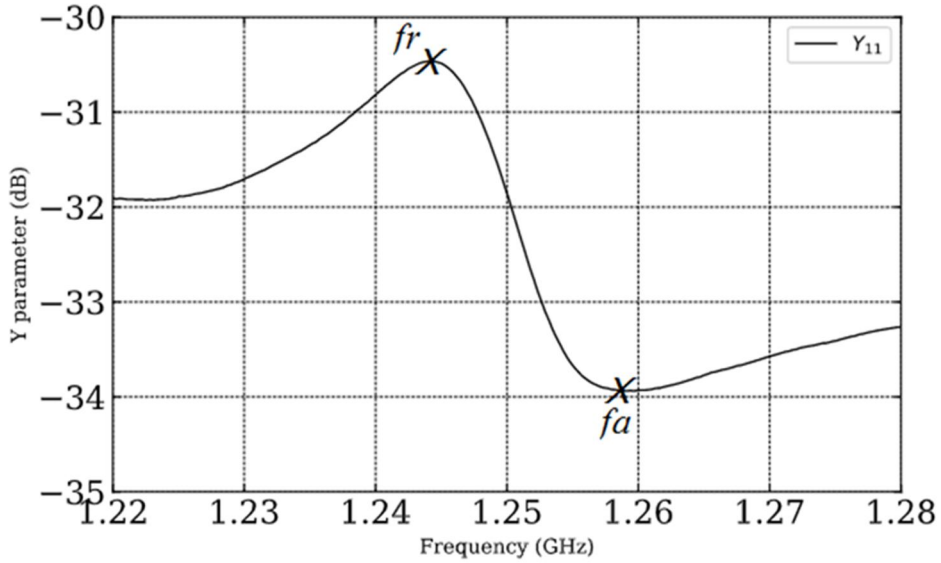

Figure 25. Resonance (*fr*) and antiresonance (*fa*) frequencies for Rayleigh mode of resonator A

Using the formula (5) previously mentioned, K^2 values were calculated for all working resonators in Rayleigh and Sezawa modes, before and after embedding the IDT. The complete data set can be seen in Table 2, while the mean change of K^2 for the resonators can be seen in Figure 26.

Table 2 Comparison of the electromechanical coupling factor K^2 for the resonators

Resonators	Rayleigh - before	Rayleigh - after	Sezawa - before	Sezawa - after
Resonator A	2.4%	2.9%	5.0%	3.8%
Resonator B	2.0%	7.9%	6.9%	6.7%
Resonator C	1.8%	8.6%	6.9%	5.8%
Resonator D	2.2%	15.9%	5.6%	10.3%
Resonator E	1.8%	6.7%	4.8%	5.4%
Resonator F	3.3%	11.1%	4.9%	9.3%
Resonator G	2.6%	10.4%	5.0%	8.0%
Resonator H	2.0%	11.4%	4.1%	8.6%

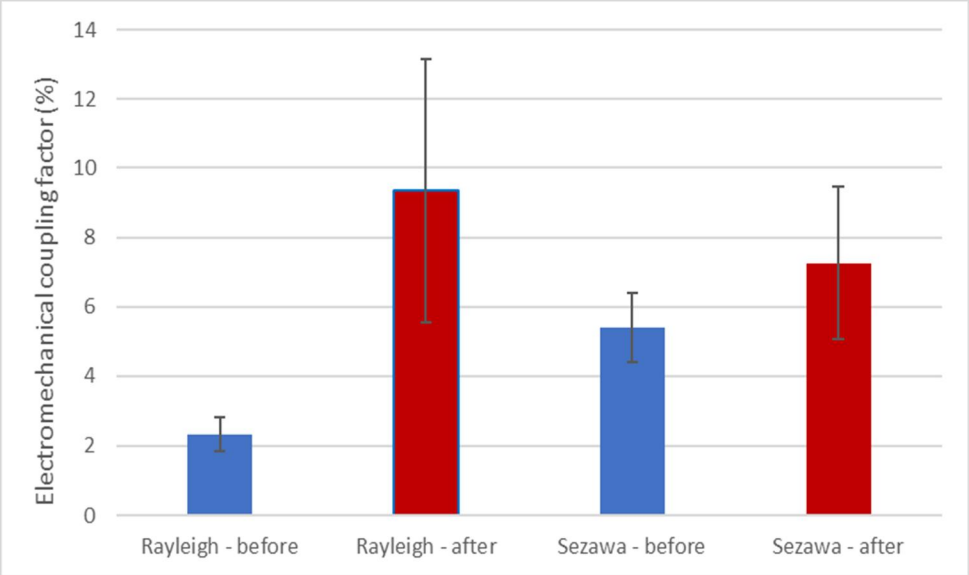

Figure 26. Average K^2 for Raleygh and Sezawa modes before and after embedding the IDT with a ScAlN thin film of 300 nm

A huge increment of the Rayleigh mode K^2 value can be observed. In this mode, embedding the IDT multiplies the K^2 value on average by 4. In the resonator with the biggest change, resonator D, it is multiplied by 7, reporting a K^2 of 15 %.

The Sezawa mode shows a significant increase as well. It is important to note that there is a correlation for resonators between the two modes. The resonators with large increases in the Rayleigh mode show an increase as well in the Sezawa mode. This is clearly positive.

After this, the six filters fabricated were measured. A Phyton script was as well used to analyze the data. The scattering parameter S_{12} vs. frequency was plotted before and after embedding the IDT in one of our filters (Filter C). The comparation can be seen in Figure 27.

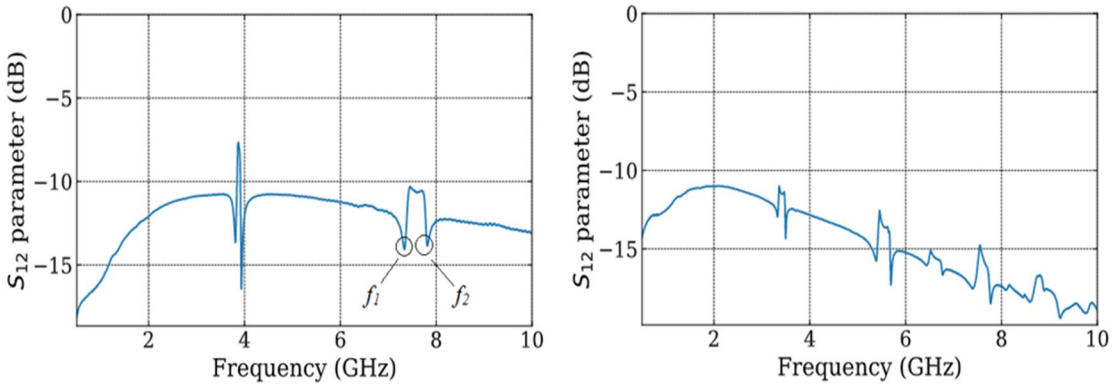

Figure 27. S12 parameter vs. frequency before and after embedding the IDT

As it is seen in the graph, embedding the IDT provokes the appearance of new modes between the Rayleigh and Sezawa modes. However, although it might have potential for the future, the two modes previously mentioned are the main focus. The bandwidth of the Rayleigh and Sezawa modes depends on the electromechanical coupling factor K^2.

Measuring the frequency range (from f_2 to f_1, as they can be seen in Figure 27) of Rayleigh and Sezawa modes the mode bandwidth of the filter can be obtained, which in turn depends of the electromechanical coupling value K^2. The bandwidth of the fabricated filters can be seen in Table 3 and in Figure 28.

Table 3 Bandwidth values for the filters (MHz)

Filters	**Rayleigh - before**	**Rayleigh -after**	**Sezawa - before**	**Sezawa - after**
Filter A	109	134	334	246
Filter B	125	175	514	353
Filter C	123	170	466	375
Filter D	150	204	594	456
Filter E	178	276	658	583
Filter F	157	334	716	643

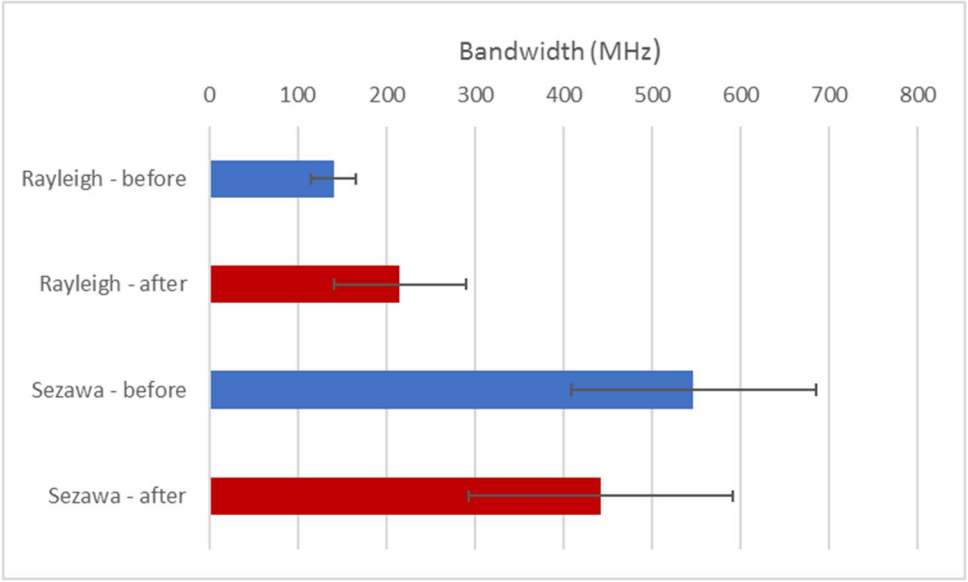

Figure 28. Average bandwidth for Raleygh and Sezawa modes before and after embedding the IDT (MHz)

The bandwidth for the Rayleigh mode improves in all the filters, following the same positive behavior than in the resonators. On average, embedding the IDT multiplies the bandwidth by 1.5. In the best case, which is Filter F, the bandwidth is doubled. This backs our resonators results and proves that not only is it possible to rise K^2 by embedding the IDT, but it is possible to link this rise to a bandwidth rise in the filters.

However, embedding the IDTs have a different effect on the bandwidth of the Sezawa mode. On average, for this mode, the bandwidth after embedding the IDT is 80% of the bandwidth the device had before. This result is not entirely unexpected. Simulations done with the embedded IDT show that for some determinate normalized thickness, embedding the IDT doesn't increase K^2. This can be seen in Figure 29. [4] [22] In the left, K^2 variation for normalized thickness is plotted for structures with embedded IDT, and in the right for structures without embedded IDT.

Although generally speaking K^2 increases by embedding the IDT according to the simulations, it is possible that for some normalized thickness the Sezawa mode goes down, while maintaining the potential to increase if this variable is changed, as it has been showed in the resonators. The experimental results cannot be compared to the dispersions curves presented in Figure 29 because these dispersion curves were simulated for Cu in the electrode. In addition, these simulation curves have a limited normalized thickness range

(0.2 to 1.2). Our filters, for example, are out of that range. However, the figures can give us information about the general pattern followed by these curves.

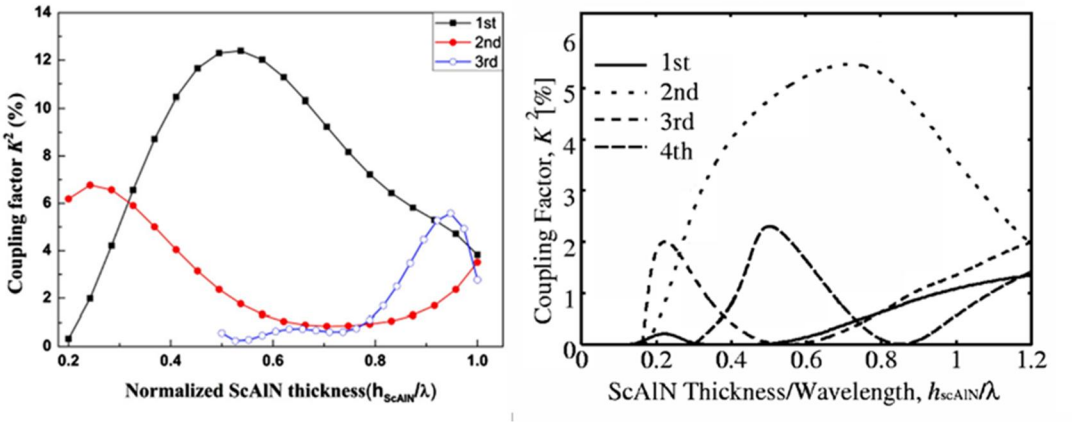

Figure 29. Variation of K^2 with normalized thickness with embedded IDT (left) and without embedded IDT (right) [4] [21]

Therefore, with the results presented in this work, the embedding of the IDT within the ScAlN thin films can be confirmed to be able to increase K^2 for the measured propagation modes which in turn increases the bandwidth of the fabricated devices.

4 Conclusions

Before starting this project, and basing our knowledge in the current literature and more concretely in the simulations done by K. Hashimoto et al., [10] it was expected to improve the electromechanical coupling factor K^2 by embedding the IDT. That was the objective of this project.

The results obtained in this project have fulfilled our expectations. It has been empirically proved that embedding the IDT rises K^2 in SAW devices and some very positive results have been obtained for the resonators. It has also been proved that it's feasible to fabricate them with this new structure.

Working filters have been fabricated with an improved bandwidth in the Rayleigh mode, which was the main incentive for improving K^2. As it was said in the introduction of this work, this improved bandwidth can serve 5G technology as well as ultra-wide bandwidth devices working in lower frequencies.

Taking all of this into account, it can be concluded that this project has achieved its goal and it could be the start of subsequent investigation in this field.

5 Future work

This project has a lot of potential for future work. This is a possible starting point for a new line of development of SAW devices. Having proved that the electromechanical coupling factor can be enhanced by embedding the IDT, other variables that affect the device performance have yet to be optimized for this new structure.

One possible optimization is to make feasible the deposition of the electrodes directly on diamond, obtaining the structure of Figure 3 right. This will improve wave velocity, as the IDT is closer to diamond. Testing the change in K^2 in this structure compared to the one that was used in this work (Figure 12) is another possible line of work.

The simulations previously referred to in this work [25] have showed that changing ScAlN and electrode thickness affect K^2 and other device properties (like the wave velocity) differently whether the IDT is embedded or not. This means that the previously optimized thickness values for ScAlN and the electrode are not the same for this new structure.

Therefore, optimizing these values is essential and it will give us even more potential for the enhancement of K^2. The decrease of filters K^2 in the Sezawa mode showed in this work can certainly be overturned this way, as an increase has already been obtained in the resonators results.

One final line of work could be to test how the sputtering conditions change the device properties. The variation in the devices K^2 could very well be due to how ScAlN has been deposited in that concrete section of the sample, although other reasons can't be discarded as it is an extremely sensible process.

Summarizing, the results of this project show great potential and have opened the possibility of a new line of development in the fabrication of SAW devices.

6 Work realized by the student

- Sputtering: the student has had an active participation in this process, learning the necessary steps to make the synthesis process.
- Wet etching: the student has designed and realized the complete wet etching experiments, managing the profilometer and the phosphoric acid etching itself, as well as analyzing and plotting the obtained data.
- Nanolitography: the student has learned this technique process, as well as the correct use of the equipment, having an active role in the deposition and development of the resists.
- Metallization: the student has learned this technique process, as well as the correct use of the equipment.
- Lift-off: the student has realized the samples cleaning and lift-off, has checked the deposition thicknesses with the profilometer and has checked the process outcume with SEM and optical microscopes.
- Network analyzing and XRD: the student has participated in these characterization techniques, understanding their mechanism as well as their purpose.
- Data analysis: the student has analyzed all data obtained from the characterization techniques, assembling the network analyzer data sets with a python script to be able to compare the properties evolution as well as plotting the necessary graphs

7 Bibliography

[1] J. G. Rodriguez Madrid, "Ultra High Frequency Thin Film SAW Devices," Universidad Politécnica de Madrid (UPM), 2013.

[2] T. Yanagitani and M. Suzuki, "Electromechanical coupling and gigahertz elastic properties of ScAlN films near phase boundary," *Appl. Phys. Lett.*, vol. 105, no. 12, p. 122907, Sep. 2014.

[3] T. Nishihara, T. Yokoyama, T. Miyashita, and Y. Satoh, "High performance and miniature thin film bulk acoustic wave filters for 5 GHz," vol. 00, no. c, pp. 969–972, 2003.

[4] Q. Zhang, T. Han, J. Chen, W. Wang, and K. Hashimoto, "Enhanced coupling factor of surface acoustic wave devices employing ScAlN/diamond layered structure with embedded electrodes," *Diam. Relat. Mater.*, vol. 58, pp. 31–34, Sep. 2015.

[5] K. Hashimoto, *Surface Acoustic Wave Devices in Telecommunications*. Berlin, Heidelberg: Springer Berlin Heidelberg, 2000.

[6] G. W. Farnell and E. L. Adler, "Elastic Wave Propagation in Thin Layers," in *Physical Acoustics*, vol. 9, no. C, Academic Press, INC., 1972, pp. 35–127.

[7] R. Guldiken and O. Onen, *MEMS ultrasonic transducers for biomedical applications*. Woodhead Publishing Limited, 2012.

[8] A. Pérez Campos, "CMOS integration of AlN based piezoelectric microcantilevers," Universidad Politécnica de Madrid (UPM), 2015.

[9] J. G. Rodríguez-Madrid *et al.*, "Optimization of AlN thin layers on diamond substrates for high frequency SAW resonators," *Mater. Lett.*, vol. 66, no. 1, pp. 339–342, 2012.

[10] Q. Zhang, T. Han, J. Chen, W. Wang, and K. Hashimoto, "Enhanced coupling factor of surface acoustic wave devices employing ScAlN/diamond layered structure with embedded electrodes," *Diam. Relat. Mater.*, vol. 58, pp. 31–34, 2015.

[11] S. Wu, M. Y. Wu, J.-L. Huang, and D.-F. Lii, "Characterization and Piezoelectric

Properties of Reactively Sputtered (Sc, Al)N Thin Films on Diamond Structure," *Int. J. Appl. Ceram. Technol.*, vol. 11, no. 5, pp. 894–900, Sep. 2014.

[12] R. C. Turner, P. A. Fuierer, R. E. Newnham, and T. R. Shrout, "Special Issue on TransducersMaterials for high temperature acoustic and vibration sensors: A review," *Appl. Acoust.*, vol. 41, no. 4, pp. 299–324, 1994.

[13] Y. Iwazaki, T. Yokoyama, T. Nishihara, and M. Ueda, "Highly enhanced piezoelectric property of co-doped AlN," *Appl. Phys. Express*, vol. 8, no. 6, p. 061501, Jun. 2015.

[14] M. Akiyama, K. Kano, and A. Teshigahara, "Influence of growth temperature and scandium concentration on piezoelectric response of scandium aluminum nitride alloy thin films," *Appl. Phys. Lett.*, vol. 95, no. 16, p. 162107, Oct. 2009.

[15] M. Akiyama, T. Kamohara, K. Kano, A. Teshigahara, Y. Takeuchi, and N. Kawahara, "Enhancement of Piezoelectric Response in Scandium Aluminum Nitride Alloy Thin Films Prepared by Dual Reactive Cosputtering," *Adv. Mater.*, vol. 21, no. 5, pp. 593–596, 2009.

[16] A. Ababneh, H. Kreher, H. Seidel, and U. Schmid, "The influence of varying sputter deposition conditions on the wet chemical etch rate of AlN thin films," *Smart Sensors, Actuators, MEMS III*, vol. 6589, p. 65890U, 2007.

[17] M. S. Lozano, Z. Chen, O. A. Williams, and G. F. Iriarte, "Temperature characteristics of SAW resonators on $Sc_{0.26}Al_{0.74}N$/polycrystalline diamond heterostructures," *Smart Mater. Struct.*, vol. 27, no. 7, p. 075015, Jul. 2018.

[18] A. Pérez-Campos, M. Sinusía Lozano, F. J. Garcia-Garcia, Z. Chen, and G. F. Iriarte, "Synthesis of ScAlN thin films on Si (100) substrates at room temperature," *Microsyst. Technol.*, vol. 24, no. 6, pp. 2711–2718, Jun. 2018.

[19] M. Sinusía Lozano *et al.*, "Piezoelectric characterization of Sc 0.26 Al 0.74 N layers on Si (001) substrates," *Mater. Res. Express*, vol. 5, no. 3, p. 036407, Mar. 2018.

[20] Fewster and M. Birkholz, *Thin Film Analysis by X-ray*. 2006.

[21] K. Hashimoto, S. Sato, A. Teshigahara, T. Nakamura, and K. Kano, "High-performance surface acoustic wave resonators in the 1 to 3 GHz range using a ScAlN/6H-SiC structure," *IEEE Trans. Ultrason. Ferroelectr. Freq. Control*, vol. 60, no. 3, pp. 637–642, Mar. 2013.

[22] K. Hashimoto *et al.*, "High Q surface acoustic wave resonators in 2-3 GHz range using ScAlN/single crystalline diamond structure," in *2012 IEEE International Ultrasonics Symposium*, 2012, pp. 1–4.

[23] B. Stasinska and A. Marcewicz-kuba, "Reactor of catalytic methane oxidation from ventilation air – from laboratory to quarter-technical scale prototype , AGH Journal of Mining and Geoengineering , Quarterly of AGH Unive ...," no. May 2014, 2012.

[24] J. Rosenbaum, *Bulk Acoustic Wave Theory and Devices (Artech House Acoustics Library)*. 1988.

[25] G. Tang, "Investigation on High Performance Surface Acoustic Wave Devices Using ScAlN Thin Films," no. January, 2017.

8 Appendix

This code was used to plot the graphs seen in 3.3. Python 3.6.8 with Anaconda version was used for this purpose.

#Comments

- For the resonators we used the following code:

#Necessary Python modules for this code are imported:

#os: Gives information about the system (to take and save archives from the system folders)

#pylab: Gives necessary code for the figures

#tkinter: Opens applet to select the folder

#skrf: The module we use to open the archives .s*p

#time: To calculate processing time

#Convertidores: To convert inches to cm

```
import os, pylab, tkinter, skrf, numpy,scipy,math,csv,operator,time
import matplotlib.pyplot as plt
from tkinter import filedialog
from mpl_toolkits.axes_grid.inset_locator import inset_axes
from Convertidores import cm2inch
from matplotlib.ticker import MultipleLocator, FormatStrFormatter
```

#Modification of some rc (pylab module standard parameters)

#lines: plot lines: size and color

#grid: grid size, color and style

#xtick e ytick: y and x-scales ticks: direction, position and size

#font: writing font

#legend: plot legend

```
pylab.rc('lines', linewidth=1.0, markersize=3)
pylab.rc('grid', linewidth=0.5, ls='--', c='k')
pylab.rc('xtick', direction='in',top='True',labelsize=16)
pylab.rc('ytick', direction='in',right='True',labelsize=16)
pylab.rc('font',family='serif')
pylab.rc('legend', numpoints=1)
```

#Detect the aproximate point where the peak is

```
def indexspoint(fs,point):
    j,s=[],[]
    for i in range(len(fs)):
        k=abs(fs[i]-point)
        s.append(k)
        j=s.index(min([abs(x) for x in s]))
    return(j)
```

#To open the file/s and list them and we introduce the IDT distance value (m)

```
def filesfork():
    IDT=2.8125*10**(-6)

Values=[('Name','PAresona','Pseries','FAresona','Fsereis','K2Rosembau
n']
    ValuesY=Values
    ValuesZ=Values
    names= tkinter.filedialog.askopenfilenames()
```

```
    listofnames=list(names)
    t=time.time()
    for i in range(len(listofnames)):
```

#Once the file is openned, to look for the admittance matrix, its minimun and maximun, and their corresponding frequencies

```
        print(listofnames[i])
        fn=os.path.basename(listofnames[i])
        fn=fn[:-4]
        device=skrf.Network(listofnames[i], name=fn[:3], f_unit='ghz')
```

#Plot each of the previous files: Admitance (Y) parameter and Spattering (S) parameter figures

```
fig=pylab.figure(figsize=(cm2inch(17),cm2inch(17/1.6180342673007837))
)
        ax=fig.add_subplot(1, 1, 1)
        device.plot_y_db(y_label='Y                          parameter
(dB)',label='$Y_{11}$',color='k')
        pylab.grid()
        pylab.xlim(xmin=1.22e9,xmax=1.28e9)
        pylab.ylim(ymin=-35,ymax=-30)
        pylab.tight_layout()
        filenameADMparameter=listofnames[i][:-4]+'_admittance.svg'
        pylab.savefig(filenameADMparameter,dpi=1200)
        pylab.close(fig)
   pylab.figure(figsize=(cm2inch(17),cm2inch(17/1.6180342673007837)))
        pylab.figure()
        pylab.title(fn,fontsize=10)
        device.plot_s_db(y_label='S          parameter          (dB)',
label='$S_{11}$',color='k')
```

```
        pylab.grid()
        pylab.ylim(ymax=0)
        pylab.legend(bbox_to_anchor=(0.99,  0.01),loc='lower  right',
borderaxespad=0.,fontsize=6)
        filenameSparameter=listofnames[i][:-4]+'_S.svg'
       pylab.savefig(filenameSparameter,dpi=1200,bbox_inches='tight')
        pylab.close(fig)
```

#Make the admittance matrix

```
        freq=device.f
        Adm=device.y_db
        S=device.s_db
        print(freq)
```

#Look for local maximum and minimums

```
        fssY=scipy.signal.argrelmax(Adm,order=125)
        fppY=scipy.signal.argrelmin(Adm,order=125)
        fs=scipy.signal.argrelmin(S,order=125)
```

#Translate it to lists

```
        fppY=numpy.array(fppY).tolist()
        fssY=numpy.array(fssY).tolist()
        fs=numpy.array(fs).tolist()
```

#Getting the list

```
        print(fppY,fssY)
```

```
        fppY1=fppY[0]
        fssY1=fssY[0]
        fs1=fs[0]
```

#Getting the values for computing

```
        fppY2=fppY1[(indexs(fppY1))]
        fssY2=fssY1[(indexs(fssY1))]
        fs2=fs1[(indexs(fs1))]
        print(fppY2,fssY2,fs2)
```

#We aproximately define the points we are interested in, in our case, between the resonance (Y_{fs}) and antiresonance (Y_{fp}) modes, and calculate K^2

```
    Points=[,]
        Yfp=[,]
        Yfs=[,]
        for i in range(len(Points)):
            fppY2=Yfp[(indexspoint(Yfp,Points[i]))]
            fssY2=Yfs[(indexspoint(Yfs,Points[i]))]
            print(fppY2,fssY2)
            print(freq[fppY2],freq[fssY2])
            K2Y=(((math.pi/2)**2)*(freq[fppY2]-
freq[fssY2])/freq[fppY2])
            ComputedY=[fn,fppY2,fssY2,freq[fppY2],freq[fssY2],K2Y]
            print(fn,fppY2,fssY2,freq[fppY2],freq[fssY2],K2Y)
```

#We finalize the code

```
    print('Done!  Files  openned:  '  ,  len(listofnames),  'in',
time.time()-t , 'seconds.')
    print('End')
errmsg = 'Error!'
tkinter.Button(text='Select      touchstone      (.s*p)      file',
command=filesfork, bg='yellow',height = 25, width = 50).pack()
tkinter.mainloop()
```

- For plotting the filters we used the following code:

#Necessary Python modules for this code are imported:

#os: Gives information about the system (to take and save archives from the system folders)

#pylab: Gives necessary code for the figures

#tkinter: Opens applet to select the folder

#skrf: The module we use to open the archives .s*p

#time: To calculate processing time

#Convertidores: To convert inches to cm

```
import os, pylab, tkinter, skrf, time
import pandas as pd
from tkinter import filedialog
from Convertidores import cm2inch
import matplotlib.font_manager
```

#Modification of some rc (pylab module standard parameters)

#lines: plot lines: siz and color

#grid: grid size, color and style

#xtick e ytick: y and x-scales ticks: direction, position and size

#font: writing font

#legend: plot legend

```
pylab.rc('lines', linewidth=3.0, markersize=3, c='k')
pylab.rc('grid', linewidth=0.5, ls='--', c='k')
pylab.rc('xtick', direction='in',top='True',labelsize=16)
pylab.rc('ytick', direction='in',right='True',labelsize=16)
pylab.rc('font',family='serif')
pylab.rc('legend', numpoints=1,)
```

#The archives we need to process are selected and converted to a list to process them in a loop

```
def RFfiles():
    t=time.time()
    names= tkinter.filedialog.askopenfilenames()
    listofnames=list(names)
    print('Files to open: ',len(listofnames))
```

#The loop obtans each archive name to open it afterwards

```
    for i in range(len(listofnames)):
```

#Open the archive to select the images

```
        if listofnames[i].endswith(('.s1p', '.s2p', '.s3p', '.s4p')):
            fn=os.path.basename(listofnames[i])
            fn=fn[:-4]
            print(fn)
            dev=skrf.Network(listofnames[i],              name=fn[:3],
f_unit='ghz')
```

#Create the images: S11, S12 and S21 paramater figures

```
            if listofnames[i].endswith(('.s1p')):


fig=pylab.figure(figsize=(cm2inch(17),cm2inch(17/1.6180342673007837))
)
                dev.plot_s_smith(draw_labels=False,
show_legend=False, linewidth=1.5, color='k')


fig=pylab.figure(figsize=(cm2inch(17),cm2inch(17/1.6180342673007837))
)
                ax=fig.add_subplot(1, 1, 1)
                pylab.title(fn,fontsize=10)


dev.plot_s_db(show_legend=True,linewidth=1.5,color='k')
                pylab.grid()
                pylab.ylabel('$S_{11}$ parameter (dB)',fontsize=18)
                    pylab.xlabel('Frequency (GHz)',fontsize=18)
                    pylab.ylim(ymax=0,ymin=-20)
                    pylab.xlim(xmax=6.0,xmin=1.5)
                    filenameSparameter=listofnames[i][:-
4]+'_S1_1.svg'
                    pylab.tight_layout()
                    pylab.savefig(filenameSparameter,dpi=1200)
                    pylab.clf()
                    pylab.close(fig)


fig=pylab.figure(figsize=(cm2inch(17),cm2inch(17/1.6180342673007837))
)
                ax=fig.add_subplot(1, 1, 1)
                dev.plot_s_db(show_legend=True,linewidth=1.5)
```

```
                pylab.grid()
                pylab.ylabel('S parameter (dB)',fontsize=18)
                pylab.xlabel('Frequency (GHz)',fontsize=18)
                pylab.ylim(ymax=0,)
                pylab.legend(bbox_to_anchor=(0.98,   0.02),loc='lower
right', borderaxespad=0.,fontsize=12)
                filenameSparameter=listofnames[i][:-4]+'_S.svg'
                pylab.tight_layout()
                pylab.savefig(filenameSparameter,dpi=1200)
                pylab.clf()
            pylab.close(fig)

fig=pylab.figure(figsize=(cm2inch(17),cm2inch(17/1.6180342673007837))
)
                ax=fig.add_subplot(1, 1, 1)
                dev.plot_s_db(0,1,show_legend=True,linewidth=1.5)
            pylab.grid()
            pylab.ylabel('$S_{12}$ parameter (dB)',fontsize=18)
            pylab.xlabel('Frequency (GHz)',fontsize=18)
            pylab.ylim(ymax=0,)
            pylab.xlim(xmin=2.0e9,xmax=3.0e9)
            filenameSparameter=listofnames[i][:-4]+'_S12.svg'
            pylab.tight_layout()
            pylab.savefig(filenameSparameter,dpi=1200)
            pylab.clf()
            pylab.close(fig)
            S12=dev.s_db[:,0,1]
            df=pd.DataFrame(S12)
            df.to_csv(listofnames[i][:-4]+'_S12.csv',index=False)
            df=pd.DataFrame(dev.f)
```

```
            df.to_csv(listofnames[i][:-4]+'_fS1.csv',index=False)
```

#We finalize the code

```
    if i==0:
        print('Done!   Files   openned:   '   ,   len(listofnames),
'in',time.time()-t , 'seconds. Time per file: ',(time.time()-t))
    else:
        print('Done!   Files   openned:   '   ,   len(listofnames),
'in',time.time()-t , 'seconds. Time per file: ',(time.time()-t)/i)


errmsg = 'Error!'
tkinter.Button(text='Select        any        touchstone        (.s*p)
file\s',command=RFfiles, bg='yellow',height = 25, width = 50).pack()
tkintermainloop()
```